# Using Prototypical Oil and Gas Sites to Model Methane Emissions in Colorado's Denver-Julesburg Basin Using Mechanistic Emission Estimation Tool

Winrose Mollel,* Daniel Zimmerle, Arthur Santos, and Anna Hodshire

*Energy Institute, Colorado State University, Fort Collins, CO, USA, 80524*

E-mail: winrose.mollel@colostate.edu

Phone: 929-247-5878

**Abstract**

Traditional bottom-up (BU) methods estimate methane emissions from oil and gas facilities by multiplying activity data with emission factors. Top-down (TD) methods measure methane emissions from all sources across an entire site and often use BU estimates to attribute emissions specifically to natural gas, often through ethane-to-methane ratio analysis. However, traditional BU methods do not adequately account for variations in throughput and failure conditions, which can significantly impact gas composition and emission rates.

The Mechanistic Air Emissions Simulator (MAES) is a computer model developed to estimate methane and other hydrocarbon emissions from oil and gas facilities. MAES employs two distinct modeling approaches: mechanistic models and traditional methods. MAES uses mechanistic models to estimate emissions based on fluid flow through equipment and equipment states, offering a detailed, process-oriented emissions representation.

In contrast, the traditional methods utilized by MAES estimate emissions by applying activity data multiplied by emission factor distributions, offering a statistical approach grounded in empirical data.

This study applies MAES to assess emission impacts on three vintages of production wellpads in the Denver-Julesburg (DJ) basin: a wellpad with two stages of separation ("old" facility), one with three stages of separation ("current" facility), and a tankless wellpad ("future" facility). The study found that increased throughput led to higher methane emissions in older wellpads but not in tankless future facilities. Additionally, MAES also showed that failure conditions, like stuck dump valves, increased emission rates and affected the ethane-to-methane ratio, which could vary by 2.15 times depending on facility configuration. These findings underscore the importance of incorporating variability in facility operations into emissions estimates to improve accuracy and guide effective mitigation strategies.

## Synopsis

Traditional inventory methods do not capture how variations in throughput and failure conditions impact gas composition and emission rates.

## Keywords

*Bottom-up inventory, Top-down inventory, Mechanistic Air Emission Simulator (MAES), Methane emissions, Natural gas*

## Introduction

Methane is the second most potent greenhouse gas (GHG), with a Global Warming Potential (GWP) of 25-28 $CO_2$e for a 100-year period.[1] As a short-lived GHG, there is increasing interest in controlling anthropogenic sources of methane, as a reduction in these emissions

could have a substantial climate impact over decadal time scales.[2] Anthropogenic methane is emitted while producing and transporting coal, natural gas, and oil. Methane is also emitted from agricultural operations, principally enteric fermentation and manure management, and from the decay of organic waste in municipal solid waste landfills and wastewater treatment.[3–5] This study focuses on natural gas, as methane is its primary component.

The natural gas supply chain is often divided into three sectors: upstream, midstream, and downstream.[6–8] Upstream operations deal with oil and gas exploration, production, and initial separation of production into gas and oil components and wastewater. Midstream operations then transport gas to gas processing plants, where the gas is upgraded to market standards. Additional midstream transmission and storage infrastructure transports the upgraded gas to consumers and provides short-term storage. Downstream operations distribute gas to consumers.

Methane is typically co-emitted with heavier hydrocarbons and volatile organic compounds (VOCs), and often the ethane-methane (C2/C1) ratio is used to attribute methane emissions between oil and gas (O&G) and other sources when performing regional estimates where emissions from multiple sources are mixed.[9,10] Peischl et al.[9,11] conducted comprehensive studies to quantify atmospheric methane and ethane emissions, specifically focusing on various natural gas-producing basins in the United States. Their research found differences in C2/C1 ratios across various basins. Notably, the Fayetteville basin had the lowest C2/C1 ratio of $0.007 \pm 0.003$ due to being a dry gas basin, with less ethane compared to methane.[12] Conversely, the Bakken basin had the highest C2/C1 ratio on the order of 0.4–0.5 as a wet gas basin, with more ethane relative to methane. A dry gas basin is a geological region where natural gas mainly consists of methane with minimal liquid hydrocarbons, while a wet gas basin contains substantial amounts of liquid hydrocarbons like ethane, propane, and butanes in addition to methane, resulting in a mix of gas and liquid components.

Researchers often use traditional bottom-up (BU) estimates, combined with ethane measurements, to attribute methane emissions to specific sources such as oil and gas activities, leveraging

the distinct C2/C1 ratios to differentiate natural gas emissions from other anthropogenic or biogenic sources.[9,11–14] Traditional BU inventory methods calculate emissions by multiplying an emission factor and activity data for each known source.[15,16] Different levels of government and international bodies require GHG inventories for regulatory and reporting purposes. For example, in the U.S., BU inventories are commonly used for GHG reporting to programs such as the U.S. Environmental Protection Agency (EPA)'s Greenhouse Gas Inventory (GHGI)[17] and Greenhouse Gas Reporting Program (GHGRP)[18] and the Colorado Department of Public Health and Environment (CDPHE)'s Annual Oil and Natural Gas Emissions Inventory Reports.[19] Internationally, the United Nations Framework Convention on Climate Change (UNFCCC) collects and manages global GHG inventories, which include data from various countries. In their simplest form, BU methods do not include variability in emission or activity data. For example, emission inventories submitted to the CDPHE or GHGRP use basic single-value emissions factors multiplied by counts of components or process activity. In contrast with regulatory reporting, scientific studies typically use extended BU methods that include probability distributions to represent the variability in emission ranges for both emission and activity data.[20,21] Some studies have additionally used statistical methods to extend or extrapolate available data to fill perceived gaps in available emissions data.[20,21]

Traditional BU methods rely on previously collected emission and activity data, typically derived from published field campaigns. These methods calculate emissions as averages for a large population of facilities over an extended period. This approach helps in generalizing emission estimates but may not capture facility-specific variations. The Intergovernmental Panel on Climate Change (IPCC) provides Tier 1 and Tier 2 activity data, which are often used as default options in many countries. Tier 1 factors are broad, global estimates based on limited data, while Tier 2 factors offer more detailed estimates based on national or regional data.[8,22] This produces several problems associated with traditional BU inventories: a poor representation of site-to-site variability in emissions; minimal scaling of emissions with the size, complexity, or throughput of facilities; and poor representation of temporal and spatial

variability that has been observed in real-world operations.[6,23–28]

Methane emissions have also been estimated using top-down (TD) methods.[4,29,30] TD methods estimate emissions by measuring atmospheric concentrations of pollutants and using inverse modeling techniques to attribute those emissions to specific sources or regions.[11,31] In some TD methods, measurements occur during short periods by observing individual plumes downwind of facilities,[29] while other techniques perform mass balance at a regional scale using multi-hour observations.[11,14,32] "Multi-hour" refers to observations conducted over several hours within a single day to capture temporal variability in emissions. "Regional scale" encompasses a broader area than site-specific measurements, typically including multiple oil and gas facilities within a defined region, but it is smaller than national or global scales.

Past studies have identified systematic differences between TD and BU estimates of basin-scale emissions.[10,27] One frequently-noted reason for the comparatively lower BU estimates is that BU emissions factors under-represent large emitters, also known as super-emitters. Since large emitters are infrequent, these events may be underrepresented in emission factor studies due to small sample sizes and the difficulty of measuring large emitters.[24,33] More detail in BU modeling, such as including probabilistic simulation of large emitters, could capture these large emitter behaviors, which are often currently not included in common BU models.

The Mechanistic Air Emissions Simulator (MAES) model (formerly known as Methane Emissions Estimation Tool (MEET)) was developed to address the two problems identified above: (a) poor representation of the frequency and variability of large emitters caused by process failures and (b) insensitivity of traditional BU methods to variability in facility throughput.[15,20]

This study investigates several aspects of TD/BU emission comparisons, using three prototypical production facilities derived from functional facilities in the Denver-Julesburg (DJ) basin. Simulating these facilities with varying throughput and failure conditions informs gaps in TD/BU estimates and suggests the advantages of more advanced modeling for these

estimates. "Failure conditions" refer to a condition where equipment does not operate as intended, for example an unlit flare or a stuck dump valve in a separator. This study is part of a larger research program, the Colorado Coordinated Campaign that carried out an intensive multi-scale methane emissions observation study in the DJ basin in northeastern Colorado (Figure S-1).[34,35]

# Methods

The objectives for the modeling in this study are to address two deficiencies from traditional inventories: not including failure conditions and variability in facility throughput. Additionally, we address how to efficiently model production complexity in a basin, i.e., how to map more than 4000 individual facilities into a set of models that can be simulated within reasonable computational and labor constraints.

For simplicity, the study focused on production well pads. Similar methods may be applied to more complex facilities, such as midstream compressor stations,[20] or simpler facilities, such as valve sets on pipelines or metering and regulation stations in distribution.

## MAES

MAES is a computer model that simulates high-resolution spatial and temporal methane, along with other hydrocarbon emissions from natural gas. MAES uses discrete event simulator (DES) and Monte Carlo (MC) methods to estimate emissions based on emission factors, activity data, and equipment behavior. Inputs to MAES include a data file detailing equipment behavior and counts, a factors file referencing emission factors distributions, and a gas compositions file with fluid compositions at different separation stages. Facility data, such as equipment counts and some operational conditions, were sourced from the 2021 Annual Oil and Natural Gas Emissions Inventory Reports by the CDPHE. The behavior of the equipment is determined by its states and the variables that influence changes in these

states. States represent the different conditions or modes that an equipment can be in at any given time; for example, a flare can have three states: operating, malfunctioning, and unlit. In MAES, all equipment is modeled using a finite state machine, meaning each piece of equipment can be in only one of several states at a time. Emission factors for compressors were derived from Zimmerle et al.'s[33] study on gathering and boosting facilities, while data for pneumatics were obtained from Allen et al.'s[36] research on pneumatics. Flare destruction efficiency data was sourced from Plant et al.'s[37] study on natural gas flares. See S-4 for a detailed description on the development of gas compositions used as MAES input.

DES is a modeling technique used to study the behavior of complex systems where events occur at distinct points in time and have significant impacts on the system state. In MAES, DES models various behavioral states as a function of time. Each new state is timestamped upon initiation, and the shift to the subsequent state depends on stochastically based real life probabilities of equipment operation. DES synchronizes events from multiple simulated pieces of equipment and records them sequentially, noting the duration of each event. Synchronization is of particular importance to emission simulation, as peak emission rates often occur when two events – such as two failure modes – occur simultaneously. Once DES has recorded the event sequence, it is further processed by a serializer. A serializer is a python-based code that decodes each event and converts it into a time series of emissions at the required time resolution.[15]

Emissions from natural gas systems and equipment behavior are inherently stochastic, meaning they exhibit randomness or variability.[38] To address this, MAES employs MC methods to assess a range of possible emissions over a specified timeframe. Through numerous MC iterations, the simulation accounts for variability by randomly sampling emission factors, activity data, and equipment behavior. In this study, we typically ran 100 MC iterations per simulation. This approach generates a range of emission scenarios rather than a single average, enhancing the understanding of uncertainty in the estimated emissions and facilitating the identification of rare events like equipment failures.[15] A detailed description of the MAES

model formerly known as MEET is available in Zimmerle et al.[20]

MAES uses two types of models:

- *Mechanistic models:*

  In this study, mechanistic models are used for failure conditions where emissions are a function of the fluids traveling through the equipment, or when it is necessary to synchronize the emissions from one source with those from another source. Mechanistic models estimate emissions by integrating equipment-specific operational states, such as failure frequency, duration, and throughput. These models are applied to scenarios like compressor exhaust, flare combustion and slip, open tank vents or hatches, and overpressure in atmospheric storage tanks. Specific failure modes are detailed in the following section.

- *Traditional methods:* This type of BU model uses activity counts multiplied by emissions factor distributions to estimate methane emissions in a given facility. To model when and for how long these emitters occur, mean time before failure (MTBF) and mean time to repair (MTTR) are used for leak probability and duration.[20] For example, traditional methods are used to estimate emissions from component leaks, pneumatic controllers, well completions, and compressor seal vents.

MAES addresses the variability in emissions by using time series mechanistic modeling of major equipment units to tie emissions behavior to the fluids (liquid and gas) flowing through the equipment and the operational state of the equipment, including key failure modes. Failure modes, commonly called 'abnormal process conditions', are often the largest emission sources on production facilities.[39] The conditions that result in abnormal process emissions are typically driven by complex physical processes based upon vessel geometry, fluid flow, temperature and pressure, gas flashing processes, and other physical and control parameters. To develop mechanistic models, these behaviors are analyzed, and all independent variables

*except* fluid flow rates are combined into a single variable—fluid flow—which serves as a useful driver for conditions affecting emissions.

For example, a failure in upstream equipment may cause large gas flows to be routed to downstream equipment that is not designed to handle that gas. Arriving gas overloads outlet flows, increases pressure, and changes flashing conditions in the vessel. If substantial enough, the excess gas and/or flash will overpressure the vessel, causing protection systems to vent gas. The goal of MAES' mechanistic models is to simplify these complex behaviors into a function of *only* fluid flow rate, while still capturing the key process conditions which result in emissions. Continuing the example, an analyst models the physical processes and identifies the flow rates at which the equipment transitions to a new emitting state – for example, the flow rate at which the vessel overpressured and started venting. The conversion to mechanistic models typically reduces non-linear behaviors to 'breakpoints' at which behaviors are likely to change. At each breakpoint, the fraction of gas flow that is emitted to the atmosphere changes depending on input variables and interaction between models.[40] The simplification from physical processes to mechanistic modeling accelerates computations, allowing MAES to simulate long durations - hundreds of years is common - to capture complex, highly variable emission behaviors.

MAES produces time series outputs at one-second timesteps. For each MC iteration, all emission events are recorded along with their corresponding duration and emission rate, creating an emission time series. From the emission time series, emission distributions and the frequency of each emitter can be extracted. The primary purpose of time-series modeling is to assure that dependencies between emissions are retained in the modeled emissions. For example, many unconventional wells are cycled between extended shut-in periods to increase well pressure, followed by shorter flow periods for production. Cycling of the well stimulates cycling behavior in all downstream equipment, causing correlated emissions behavior across many equipment units at the well pad. This type of correlated emissions is not typically represented in traditional BU modeling, and the associated variability in emissions is lost or

poorly represented.

Simulating a facility in MAES with and without a failure mode, or with varying throughput, supports sensitivity analysis for emissions driven by the frequency and severity of a failure condition. The following example illustrates how MAES addresses large emitters caused by failures of key components on equipment. Referring to Figure S-2, separators - an equipment used to separate the different components of a well stream, which typically includes oil, gas, and water - have dump valves.[41] Controllers driving these valves use a float in the tank to sense fluid level, then open periodically to control the liquid level in the separator. In proper operation, the controller and dump valve drain the fluid without allowing the gas to escape through the valve. A typical failure mode in a separator is a 'stuck dump valve', where the valve does not close entirely due to the buildup of deposits, a controller failure, or corrosion. In this case, all liquid is forced from the tank, and high-pressure gas will escape downstream from the equipment labeled as C (low-pressure separator) to either D (water storage tank) or E (oil storage tank). Since atmospheric product storage tanks are rated for low pressures, the additional gas may overpressure the tank and actuate a pressure relief valve (PRV) on the tanks to vent gas to atmosphere.

MAES simulates this failure by modeling the frequency (probability) of a stuck dump valve and the fraction of gas lost through the valves when stuck open. Both of these parameters can be estimated from field data. Tank overpressure is modeled by setting limits to the volume of gas that can be vented through the tank battery's exit vent piping; if gas exceeds threshold limits, a PRV opens. This mechanistic method effectively replaces a complex physical process with simpler mechanistic drivers that provide a computationally efficient, realistic, simulation of complex physical behavior.

To extend the previous example, if separator with the stuck dump valve is fed by cycling wells, fluid arriving at the separator will vary between 'on' production periods and 'off' non-production periods. Emissions through the dump valve will respond as the well cycles on/off. Therefore, an emission source which is large on average, appears as periods with

even larger emission rates (when the well cycles on), interspersed with zero emission periods (when the well cycles off). While both traditional and mechanistic models could simulate such a failure and produce the same average emissions, only mechanistic modeling captures the temporal variability in the emission source, resulting in more representative probability distributions of emission rates. As a result, the MAES BU model estimates not only the long-term average emissions but also the variability in emissions. Since MAES simulates at the same time scale as an aerial survey, MAES results can be directly compared on a probabilistic basis with estimates collected by aerial methods.

## Failure Modes

Since failure conditions may result in large emitters that account for more than half of total emissions in a basin, mechanistic modeling focuses on simulating failure modes.[29,42] Key mechanistic failure models implemented in MAES include:

1. *Stuck dump valve (SDV):* When a dump valve operates normally, all gas passes to the sales pipeline and all liquid goes to appropriate equipment downstream. When a dump valve is stuck open, a fraction ($x\%$) of the gas in the vessel is passed to downstream equipment, $(1-x)\%$ of gas is passed to the sales pipeline, and all liquid goes downstream. A stuck dump valve does not directly create emissions. However, since downstream equipment often cannot handle the excess gas, these failures may overpressure downstream tanks or other equipment, causing gas to be vented through a PRV.

2. *Tank battery PRV actuation:* Atmospheric tanks are equipped with one or more PRVs to prevent tank rupture in an overpressure condition. The mechanistic model used in this study is driven by the rate of gas entering the tank from upstream and flashed in the tank. When total gas flow exceeds a threshold level, the PRV opens to vent gas to atmosphere. The PRV will stay open until incoming gas falls below that threshold.

Since fluid flows may be highly variable, PRV actuation may also be highly variable.

While this study focuses on tank PRVs, these devices are present on all vessels at well pads, and will actuate in similar conditions on that equipment.

3. *Tank battery vent failure:* As a mechanical device, a PRV may 'stick' open with minimal stimulus from upstream fluid flows. For example, deposits may accumulate on the working mechanism or a seal may degrade. When the vent fails, the tank stays open to atmosphere and any gas in tank will escape to the atmosphere. Typically, the failure continues until personnel detect and repair it.

4. *Tank thief hatch left open:* Most atmospheric tanks have an access port used to gauge liquid levels in the tank, colloquially known as a 'thief hatch.' Thief hatches serve two purposes. First, thief hatches can be manually opened to provide access to the interior of the tank If an opened hatch is not closed after use (thief hatch left open), the tank is open to atmosphere, leading to emissions.

5. *Thief hatch pressure relief activation:* Second, thief hatches contain features to provide backup pressure relief if the tank's PRV fails to actuate in an overpressure situation. Depending upon design of the hatch, if pressure relief features actuate, the hatch closes automatically when pressure reduces *or* the hatch remains open until personnel identify the problem and close the hatch. Emissions due to automatic open/close is captured in the *Tank battery PRV actuation* model. Emissions due to automatic open/remain open, are captured in this model. Automatic closure designs are more common due to safety concerns. They prevent prolonged venting and minimize emissions.

## Sample Facilities

The MAES model can estimate emissions from either a single facility or multiple facilities in a geographic area.[20] Current data indicate the DJ basin has approximately 20,000 actively producing wells supported by 4,000-5,000 wellpads.[43] The wells and wellpads in the DJ

basin have common features based upon age, company, regulation requirements. Through multiple working sessions and data exchanges with Colorado Coordinated Campaign partner operators, 26 common prototypes representing production facility configurations, called prototypical sites (PSs), were developed (see S-3 for a detailed description of how the PSs were developed).

Three sample facilities based on the PSs developed for the DJ basin but explicitly simplified for this study were selected to demonstrate how MAES addresses the deficiencies of traditional inventory methods. These facilities represent an 'older' facility, a 'current' facility, and a state-of-the-art 'future' facility model. The models were designed to illustrate the evolution of production facility design in the DJ basin from 2000-2020; a similar evolution has occurred, and is ongoing, in other U.S. production basins.

The *old* facility is a wellpad with two stages of separation and atmospheric storage tanks for water and oil (Figure 1).

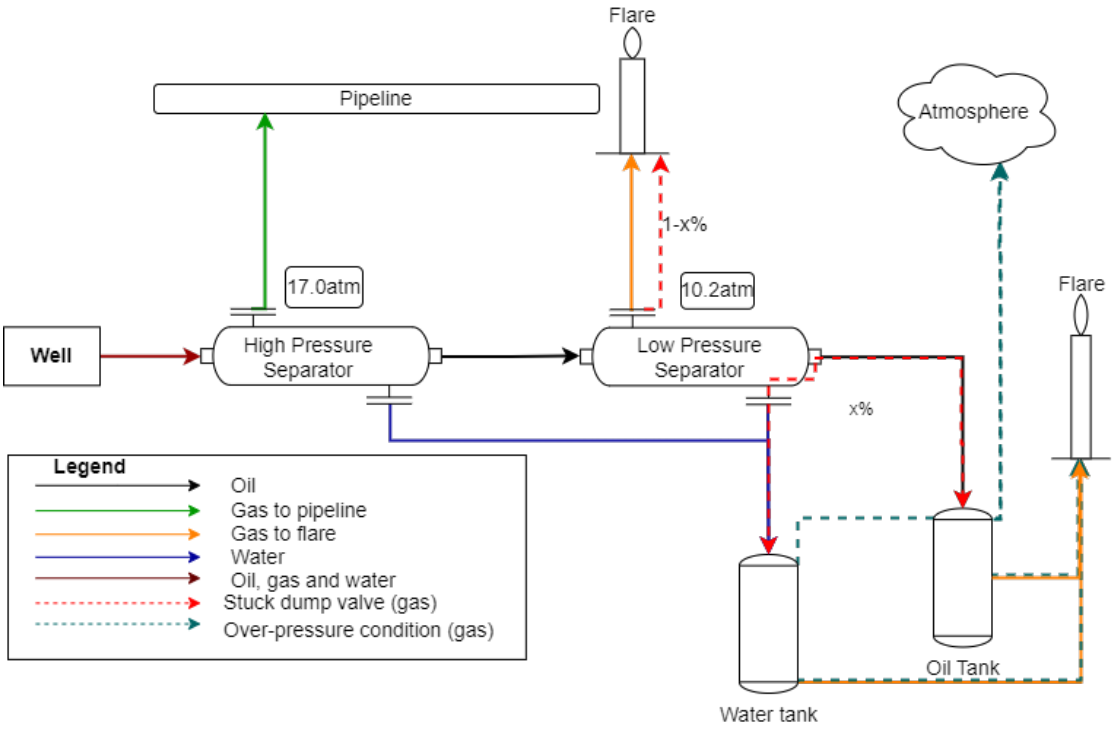


Figure 1: Facility diagram representing an old facility with an example of a stuck dump valve failure condition.

The *current* facility is a wellpad with three stages of separation (Figure 2) and storage tanks.

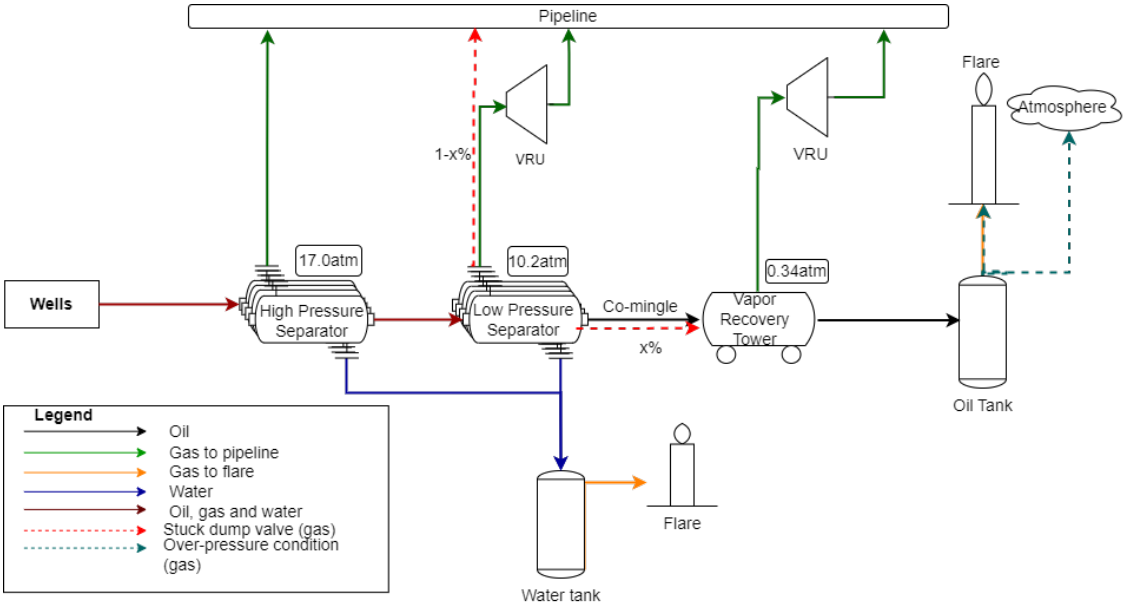


Figure 2: Diagram representing a current facility with an example of a stuck dump valve failure condition.

A *future* facility is a tankless wellpad with three stages of separation (Figure 3) and no atmospheric storage tanks (i.e. a 'tankless' facility); oil and gas are both transported from the facility using pipelines.

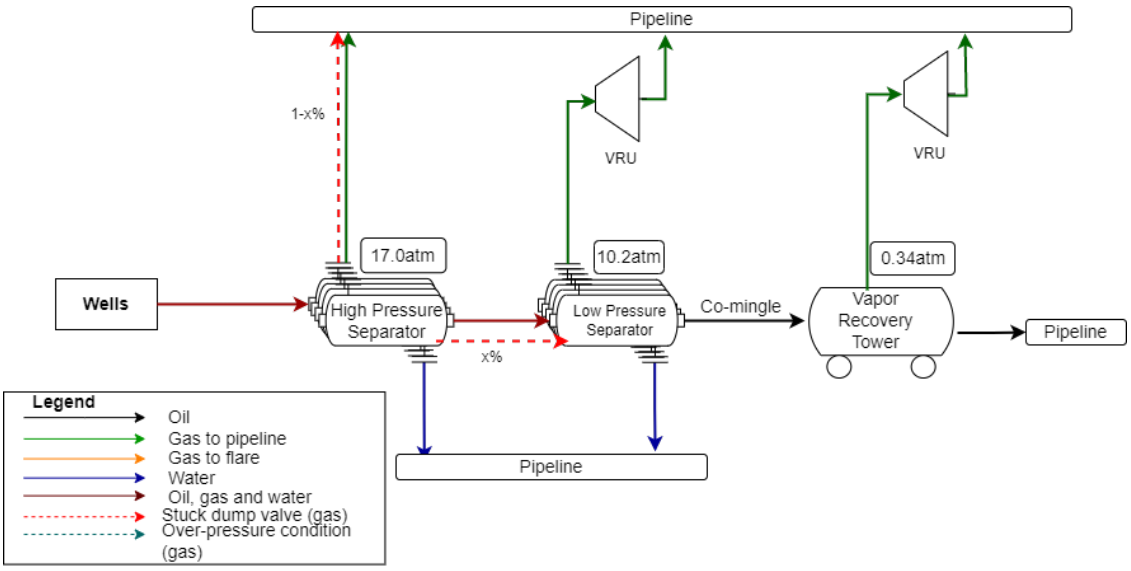


Figure 3: Diagram representing a future facility with an example of a stuck dump valve failure condition.

For a comprehensive understanding of the old, current, and future facilities, please refer to S-3.1 for detailed descriptions.

Failure modes rates, and throughput were varied to examine their impact on the facility emissions. Flow of fluids due to stuck dump valve failures are shown in Figures 1-3. Although field facilities would vary in the number of wells, all sample facilities were simulated with the same number of wells, baseline failure rate, and baseline production to support inter-comparisons. Therefore, a single 'old' facility represents the averaged emissions of multiple older well pads, while a 'future' facility configuration, based on representative equipment counts rather than the total equipment present in an actual future facility, captures only a fraction of the emissions from a complete 'future' well pad. The simulations were run for 365 days and 100 MC iterations - representing 100 years in common.

# Case Studies

MAES can be used for a plethora of analyses, including simulations of field campaigns, inventory program evaluation, analyzing changes to improve emissions, or processing overflight

data. MAES can simulate a number of different facility prototypes, allowing for efficient modeling of large regions, such as basin scales (See S-3 for more details). We use three PSs, an old, current, and future facility to address two deficiencies from traditional inventories (a)throughput analysis and (b) failure modes analysis posed earlier. The data for these facilities was obtained from Colorado Coordinated Campaign partner operators and modified to demonstrate scaling of throughput and increased frequency of failure.[34] All box plots used below show the box as the inner two quartiles, the whiskers are lines extending above and below each box (1.5 times the inter-quartile range) and the outliers are observations beyond the whisker length.[44]

## Throughput

MAES was used to show that for the same facility, changing throughput changes emission profile, a behavior that is not captured in traditional inventory methods. The demonstration varies facility throughput by simulating the baseline (original facility's water and oil production rate) production rate multiplied by 0.5, 1, and 2.

Increasing throughput increases methane emissions for the old and current facility, but not the future facility (Figure 4). Eliminating atmospheric tanks for oil (and possibly water) and the associated control flares from the future facility lowers the corresponding risk from overpressure events and thief hatch failures. Lacking these failure modes, all variation in emission rates was due to random variations in non-mechanistic emitters (i.e. emission factor based emitters). Removing tanks reduces the need for flares and onsite compression, reducing capital costs and air permitting requirements. However, savings in costs are offset by extending pipelines, equipment to stabilize oil sufficiently for pipeline transport, and bringing in grid electricity.[45]

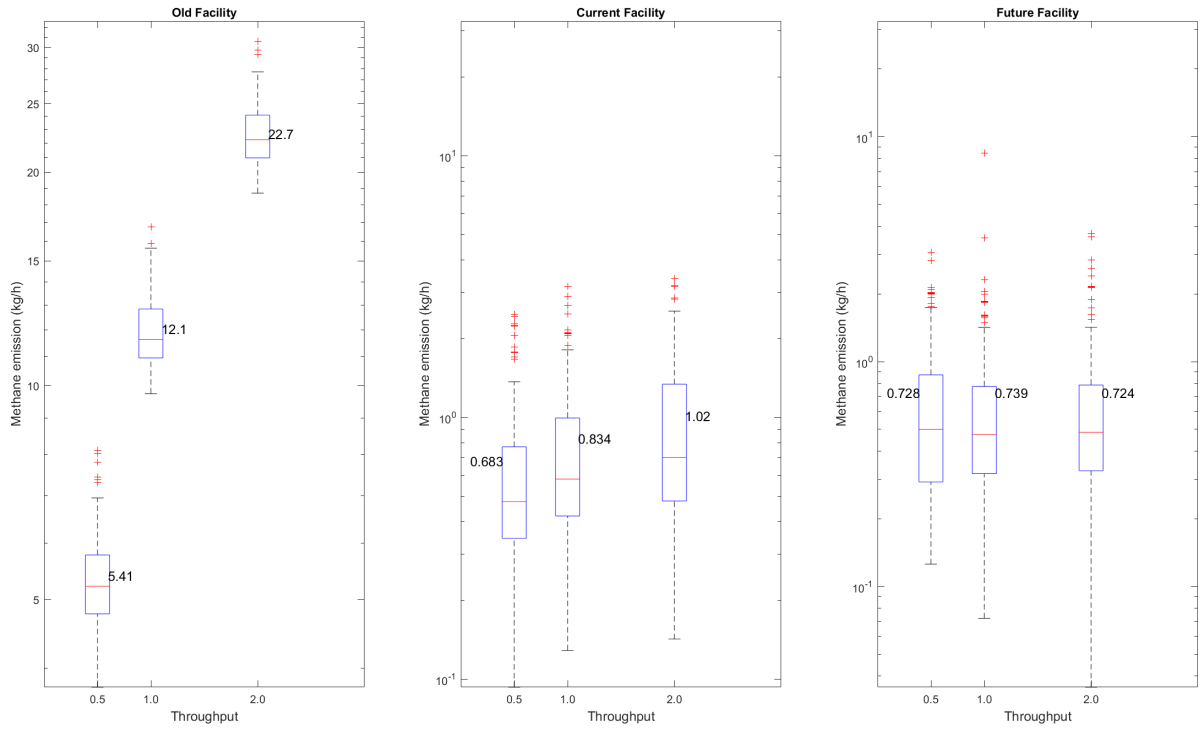


Figure 4: From left to right, the effect of changing the throughput for old, current, and future facility, respectively. An increase in throughput corresponds to increase in methane emissions for the old and current facility but not the future facility. The number on the box plots shows the mean methane emission.

While the current facility does not eliminate atmospheric tanks, it has vapor recovery units (VRUs) connected to the second and third stages of separation to compress the gas and send it to the sales line; only the storage tanks have flares for tank vapors. As a result, fewer emissions are directed to flares, and there is less risk of atmospheric emissions due to problems with the flare or equipment upstream of the tank. In contrast, the old facility has a flare connected to the second stage of separation and storage tanks. Gas composition files for all three facilities were calculated and used as an input for MAES (see S-4 for a detailed description on how the table was generated). As seen in Table 1, the total amount of vapor mass from the final stage of separation before the tank sent to the flare in the old facility is 21.8 times higher than in the current facility.

Table 1: Pressure, amount of gas, and C2/C1 ratio for all stages of separation separators and tanks across old, current, and future facilities. These parameters represent the gas compositions used as MAES input to estimate methane and ethane emissions

| | 1st stage of separation | 2nd stage of separation | 3rd stage of separation | Tank |
|---|---|---|---|---|
| **Pressure (atm)** | | | | |
| Old | 17.0 | 10.2 | N/A | 0 |
| Current and Future | 17.0 | 10.2 | 0.34 | 0 |
| **Vapor Mass ($m^3/m^3$)** | | | | |
| Old | 7,500 | 7.64 | N/A | 35.1 |
| Current and Future | 7,375 | 7.51 | 29.1 | 1.61 |
| **Ethane-Methane ratio (-)** | | | | |
| Old | 0.31 | 0.47 | N/A | 1.97 |
| Current and Future | 0.31 | 0.47 | 1.89 | 4.23 |

In Figure 4, outliers, indicated by red crosses represent data points that lie outside the inter-quartile range times 1.5. Since non-mechanistic emitters estimate emissions using emission and activity data distributions, variations between MC iterations are due to the selected emission and activity data from emission factor distributions. For mechanistic emitters, outliers in a given MC run are primarily attributed to equipment malfunctions or failures. Taking flare as example, operation of the flare is characterized by 'destruction efficiency', the fraction of gas that is fully oxidized by the flare. During the operating state, the flare operates normally, and the gas is combusted at the flare's design efficiency of 98%. When the flare malfunctions, combustion continues, but destruction efficiency drops; for this study we assume an efficiency of 90%. For all MC iterations, the same probability of failure is used, but the timing and duration of failures varies substantially between iterations. As a result, when malfunctions occur in an MC iteration, methane emissions increase, creating the outliers in Figure 4. Figure S-7 illustrates a typical flare failure scenario, using one MC iteration on the current facility.

Figure 5 categorizes methane emissions modeled mechanistically and by using emission factors. MAES models flares, tanks, and VRUs mechanistically, simulating emissions behavior that depends upon the gas flowing through these units. Flow, in turn, depends on the

throughput of the facility. While simulated failure rates are the same, the *current* facility exhibits lower emission rates than the *old* facility because less gas is routed to flares and VRUs. In contrast, the future facility holds all gas in pressurized vessels, and lacks these failure modes.

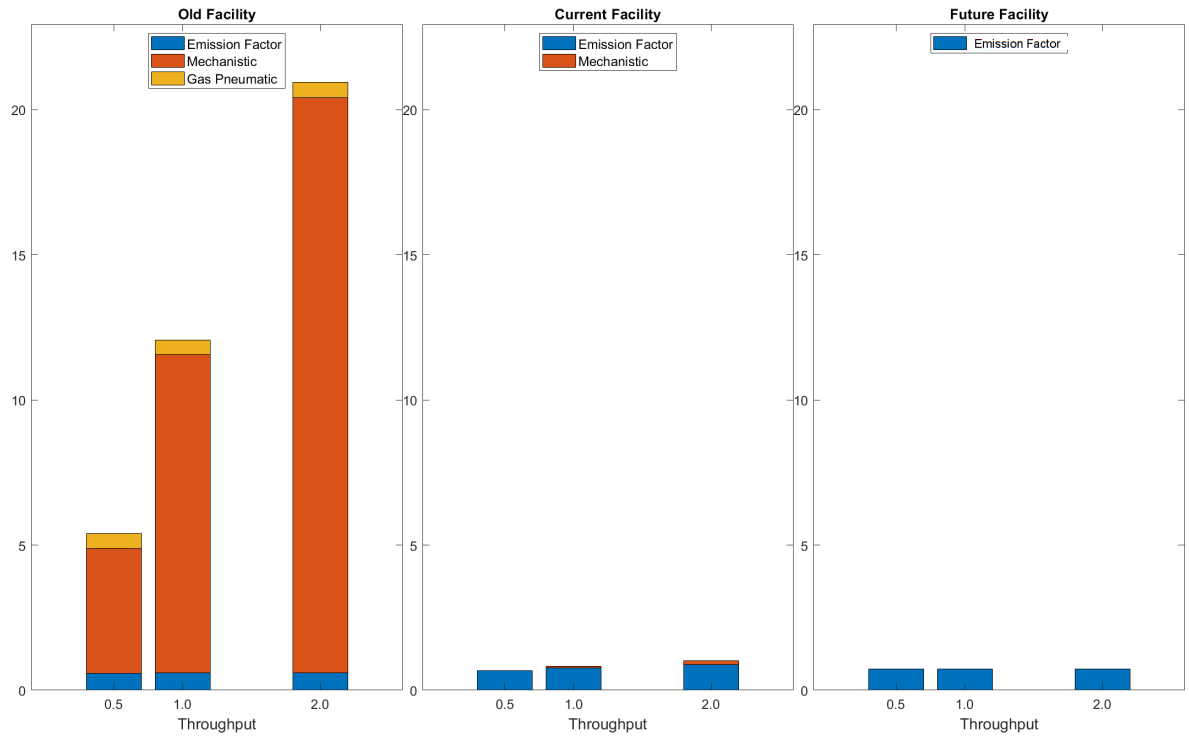


Figure 5: Mean emissions by facility type and throughput. Blue bars represent typical emissions modeled using traditional emission factors. Orange bars represent emissions from failure conditions modeled as mechanistic emitters from flares, tanks and VRUs. Yellow bars represents emissions from gas pneumatics. While simulated failure rates are the same, the *current* facility exhibits lower emission rates than the *old* facility because less gas is routed to flares and VRUs. In contrast, the future facility holds all gas in pressurized vessels, and lacks these failure modes.

Modeling throughput with associated failure modes is of interest to regulators and other stakeholders, as failures are not usually reported in traditional inventories. We examine three key examples of interest:

First, the current facility has more components than old facility. Using the traditional BU approach of activity (component count) multiplied by emission factors, the current facility designs would be expected to have a higher emission rate than the old facility.

Second, regulatory modeling often assumes historical facility designs – i.e. the old facility type – using traditional BU methods that do not include the common failure modes such as stuck dump valve and flare malfunctions modeled here.[46] As a result, the impact of throughput-driven emission modes is often not reflected in the analysis, and the true emissions from older, simpler, designs are underestimated relative to new facility designs.

Finally, while this simulation does not model every possible failure mode, it does reflect high-impact failure modes and the lower probability of failure for tankless facilities. It is important to therefore to describe why tankless facilities lack the modeled failure modes *and* have a lower probability of other failure modes with similar emission rates. Tankless designs keep all production in pressurized vessels that are pressure-rated and typically smaller than atmospheric tanks. Higher pressure provides more static head - the pressure exerted by a fluid column due to gravity- to move fluids through production processes, eliminating a variety of failure modes exacerbated by small pressure differentials, such as back-pressure problems due to the small pressure difference between an atmospheric tank and its control flare. Additionally, pressure-rated vessels tolerate more pressure variation, allowing time for controls to react, and these higher pressures are more easily sensed, making controls easier to implement. As a result, control systems are both required to operate safely and can be implemented to sense failure conditions (e.g. overpressure at any stage, insufficient oil stabilization, etc.) and shut in the facility. Therefore, tankless operation by itself does not represent a breakthrough in emissions. Rather, the operational conditions in tankless systems are more amenable to process controls and remove some failure modes known to have high emissions. However, these improvements come at a cost: These facilities require more sensing, more sophisticated facility operation, full liquid and gas pipeline networks, and often need grid electricity. These factors may not be accessible to all companies in all production regions.

## Failure Modes

Although in Methods section five failure modes were described, this study chose one failure mode, SDV, to demonstrate that even a single failure mode can have a significant impact on emissions observed from a facility. For this analysis, we focus on SDV failure rates for *old* and *current* facilities configuration. The *future* facility is not included, since the tankless design responds differently to uncontrolled gas flow from higher to lower pressure vessels (see end of previous section). In both the old and current facility, this failure condition was simulated by setting the frequency of the SDV to occur once a year for each separator on the last stage of separation before the tank. The simulations were run for 365 days with 100 MC iterations. This analysis focused on a single MC run to show in detail the mechanism and effect of the SDV failure mode.

For the current facility operating normally, any gas flashing in an atmospheric tank is routed to a flare. The pressure differential from an atmospheric tank to a flare is low, typically $<$ 1 psi (7 kPa). Since this pressure differential must drive gas flow through all piping runs, flame arresters, valves, and other restrictions, the amount of gas that can be sent to the flare without overpressuring the tank is limited. When SDV occurs on the final separation stage prior to an atmospheric tank, some or all of the gas flashed at that stage is diverted from the pipeline to the tank. Given the low pressure differential, pressure in the tank cannot rise far enough to push the incoming gas to the flare, which increases pressure in the tank and causes the tank's PRV to open.

MAES translates this complex behavior into mechanistic model driven by fluid flow. For example, the current facility flare is designed to handle 1000 scfh whole gas (470 slpm). Referring to Table 1, the total flash per well is 9 scf/bbl $\times$ 46.5 bbl/h, or 420 scfh (200 slpm). If 40% of third stage gas escapes a stuck dump valve to the tank, total gas flow exceeds 3000 scfh (1415 slpm). Since the tank-flare system is capable of handling 1000 scfh, the excess 2,000 scfh of gas ($\approx 3.2 \frac{kg\ CH_4}{h}$) will vent to atmosphere through the tank's PRV.

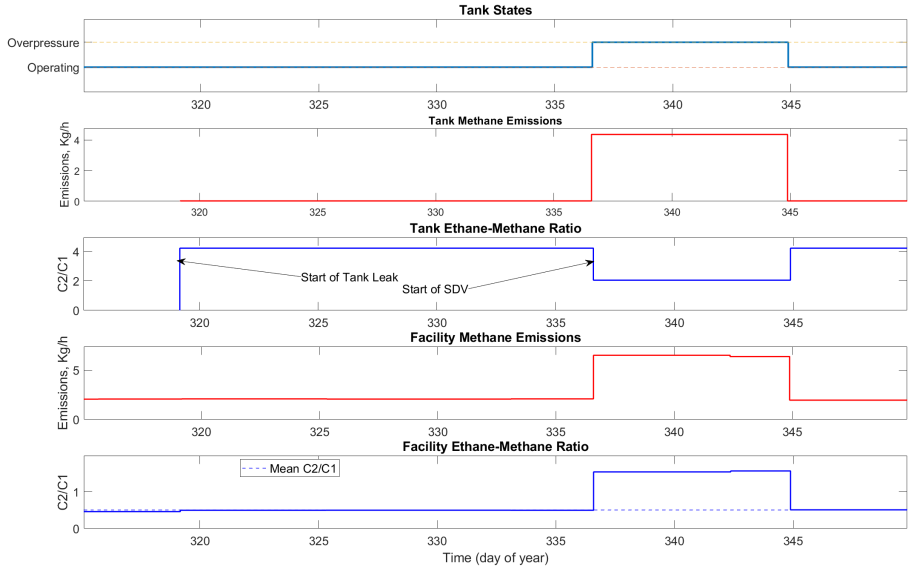


(a) Current facility

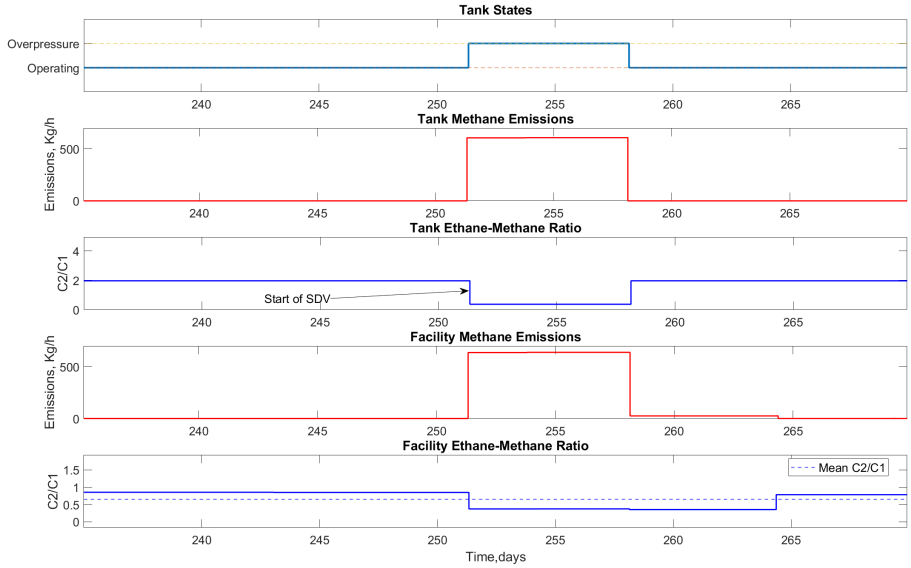


(b) Old facility

Figure 6: Effect of tank leaks and a SDV on tank and facility emissions for one MC iteration. For the current facility, panel (a), a leak starts on day 319, on the tank, releasing some of the flash gas from the tank. The gas has a high VOC content, including ethane, resulting in a high C2/C1 ratio but a relatively low emission rate. At day 336, the third stage dump valve sticks open, routing a fraction of the lower C2/C1 ratio third stage flash gas to the tank, causing the tank to overpressure and vent to the atmosphere. While the leak has minimal impact on the current facility emission rate, the SDV impacts both emission rates and C2/C1 ratio for the facility. Similarly, for the old facility, panel (b), at day 351, second stage dump valve sticks open, routing a fraction of lower C2/C1 ratio second stage flash gas to tank, causing the tank to overpressure and vent to the atmosphere. The impacts of SDV on emission rate and C2/C1 ratio are more significant on the old facility compared to the current facility.

As shown in Table 1, the gas from the third stage of separation has more methane relative to ethane than the gas flashed in the tank. When a dump valve is stuck in the third stage of separation separator, some fraction of gas from the third stage of separation separator goes to the tank. For both PSs, the C2/C1 ratio decreases during an overpressure event (third panel on in Figure 6). However, for the old facility, this facility C2/C1 ratio drops with the SDV, as a result of a very large emission rate, due the amount of gas flashed in the first stage of separation. Therefore, old facility emission rate and C2/C1 ratio are significantly different than the current facility, even though both facilities are driven by the same well production rates and characteristics.

## Implications of C2/C1 ratio on methane source attribution

Methods like aerial or drive-by surveys provide snapshots of emissions data over brief periods, which can be challenging to incorporate into the broader context of annual reporting. By using mechanistic models, these short-term measurements can be integrated into a more comprehensive analysis, ensuring that the variability and transient behaviors observed during these surveys are accurately reflected in the long-term emission estimates.

For this analysis, we focus on stuck dump valve failure rates for the current facility configuration, as there is more data available for stuck dump valves on current facilities.[47] The frequency of the stuck dump valve was set to happen once per year for each separator. We assume a driving and aerial mass balance survey using methane and ethane detecting equipment.

### Driving Survey

Emissions from the current facility were simulated for 365 days with 500 MC iterations where each MC iteration represents one facility, and we present instantaneous methane emissions and C2/C1 ratio for 500 current facilities. This simulation demonstrates a problem in the facility that releases a large amount of gas in the early stages of separation. For this study,

a stuck dump valve failure mode mechanism was used to study the effect of the failure on emissions and C2/C1 ratio.

Figure 7 shows methane emissions in kg/h as a function of C2/C1 ratio. The curved shape of the graph is because methane emissions decrease more rapidly through stages of separation compared to ethane. The routine emissions are characterized by low instantaneous methane emissions with a wide range of C2/C1 ratios since MAES simulates routine emissions at each major equipment on each stage of separation. However, some emission factors distributions are long tailed, such as the VRU component leak emission factor distribution - obtained from a gathering and boosting study.[33] At some point during the simulation, a VRU component leak emission factor gets picked from the tail of the distribution resulting in high instantaneous methane emissions during that MC run; shown by the black box in Figure 7. During a stuck dump valve failure mode when the tank is in overpressure, high instantaneous methane emissions corresponding to C2/C1 ratio of between 1.10 and 2.10 are observed (shown by the red box on the plot) compared to low routine emissions associated with C2/C1 ratio between 0.31 and 4.23.

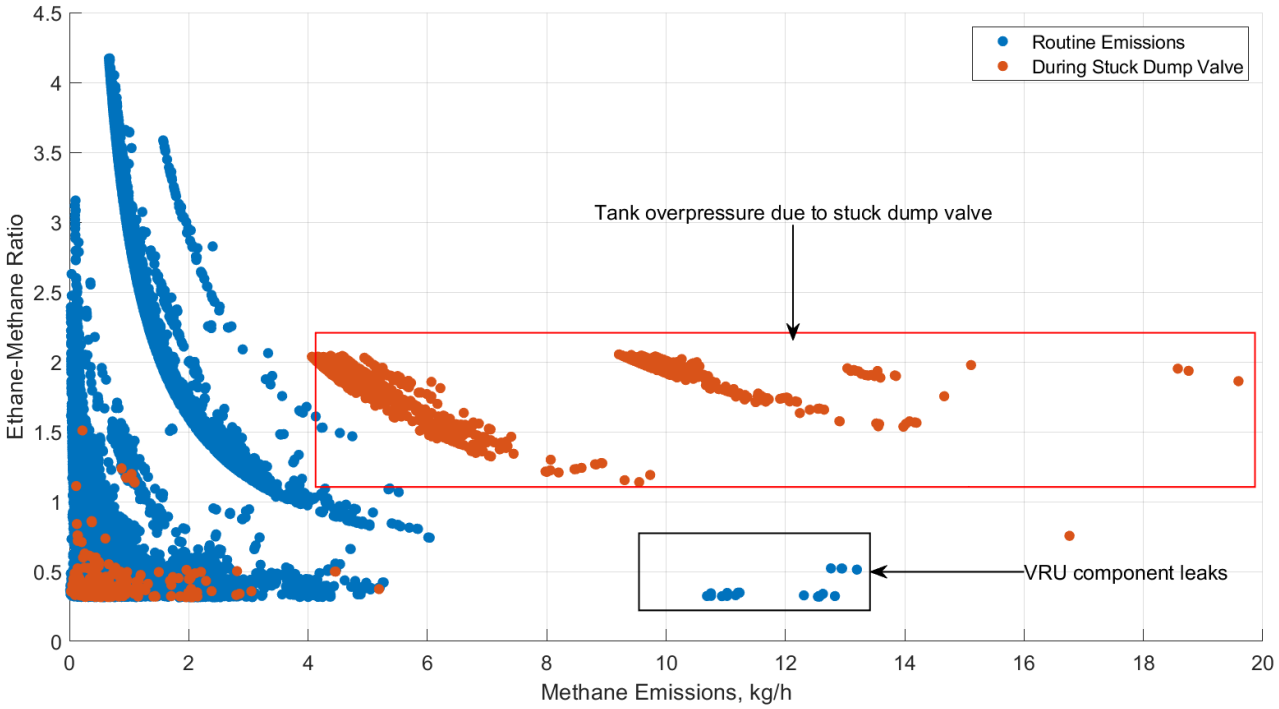


Figure 7: Current facility instantaneous methane emissions in kg/h against C2/C1 ratio. The red box shows methane emissions and the corresponding C2/C1 ratio due to tank overpressure as result of stuck dump valve. The black box shows VRU component leak emissions.

Figure 7 demonstrates a method that could be used during a driving survey to evaluate the status of the facility. If the site configuration from a given basin is known reasonably well, a driving survey with a methane-ethane instrument should be able identify not only that large emission event is taking place, but also classify likely causes of that large emitter. For example, during a driving survey in the DJ basin in a facility with the same configuration as the current facility, if high methane emissions and C2/C1 ratio between 1.10 and 2.10 are observed, it should indicate that there are early stages of separation failure occurring in the facility.

## Aerial survey

To compare with aerial mass balance flights – a form of TD measurement – simulated emissions must be made comparable to air mass sampled by the aircraft downwind of the

basin. In the DJ basin, a typical transport time for an emission plume across the basin, influenced by prevailing winds, is approximately 4 hours. This time frame is based on average wind speeds and applies to the distance that emissions are likely to travel under normal atmospheric conditions. Therefore, to simulate the air mass seen by the aircraft, data are block-averaged to 4 hours. Each MC iteration represents one year for one facility; these emissions were block averaged to four-hour periods, resulting in 2190 emission estimates for each facility. Summing each 4-hour period across the 500 MC iterations provides 2190 time-average emissions for 500 similar facilities. While this facility count is smaller than the DJ basin as a whole, it is sufficiently large to illustrate shifts in C2/C1 ratio.

As seen in Figure 8, the 4-hour average C2/C1 ratio for a case with a stuck dump failure mode was higher than cases with a stuck dump failure mode. The 4-hour average C2/C1 ratio during normal routine emissions for the current facility is around 0.91 but 1.69 during a stuck dump valve failure mode.

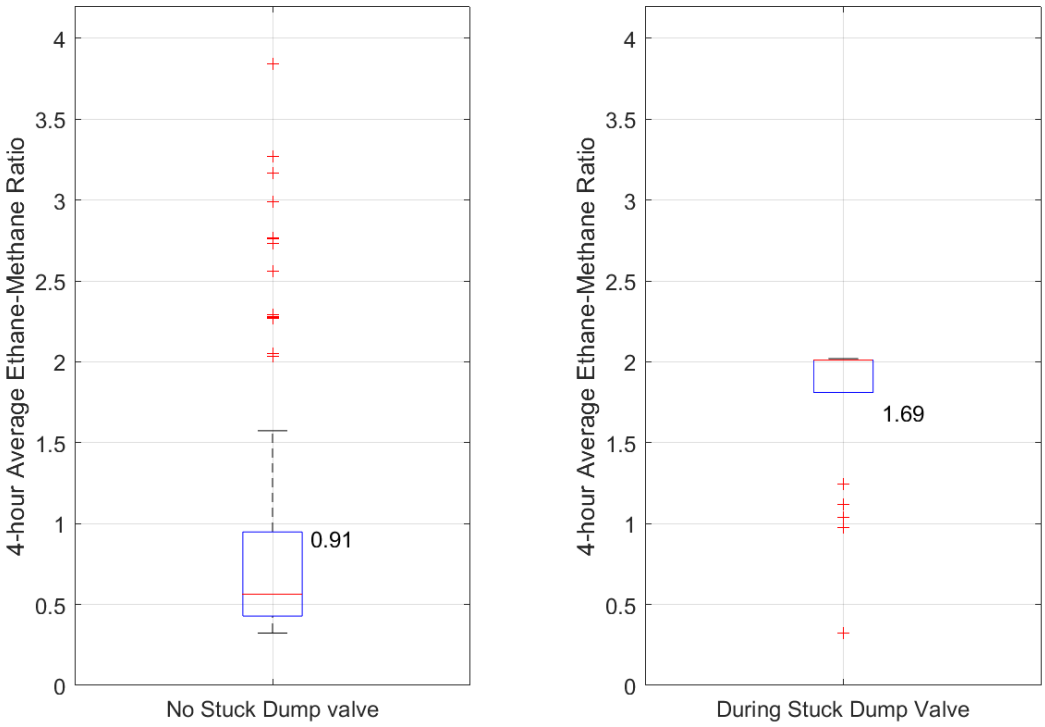


Figure 8: 4-hour average for C2/C1 ratio for the current facility during normal routine emissions and an Overpressure event. The average C2/C1 ratio increase during stuck dump valve failure mode.The number next to the boxes represents the mean.

During aerial measurements, changes in C2/C1 ratio could inform on the failure modes on the facilities being surveyed. In this case, any failure in the early stages of separation before the tank would result in a higher C2/C1 ratio than during routine emissions. MAES could be used as a diagnostic tool on failure models effect on C2/C1 ratios for correct methane source attribution for TD measurements.

## Conclusion

This study demonstrates how mechanistic modeling addresses two key deficiencies in traditional BU methods: facility throughput variability and failure modes. Mechanistic models enhance simulation accuracy, supporting design decisions like evaluating emissions trade-offs between adding separation stages or vapor recovery units versus flaring, or reducing emissions by

excluding atmospheric tanks in new facilities.

By incorporating multi-species modeling, these simulations capture the behavior of equipment under diverse conditions, providing essential data for downstream analyses, such as C2/C1 ratios for basin-scale attribution or facility-level failure assessments. Mechanistic models also integrate short-duration, facility-scale surveys into long-duration estimates for annual reporting, translating survey-detected failures into data on failure frequency, duration, and emission rates—key for reconciling TD and BU emissions estimates.

To be practical, mechanistic modeling must scale to basin-level complexity. This involves using automated tools and representative sites to classify facilities accurately by design. For example, with over 4,000 production sites in the DJ basin, modeling each individually would be costly and inefficient. Instead, prototypical sites reduce the effort by limiting simulations to key facility types, each modeled across different well counts and throughput rates.

Mechanistic models face limitations in balancing simulation fidelity with computational efficiency. Simplifications are often necessary and must be carefully validated. Modeling all emission sources is also impractical; for example, MAES currently does not model working flash—the flash and evaporation that occur when hydrocarbon liquids are stored for extended periods (days). This omission is usually negligible for newer facilities, where liquids do not remain in atmospheric tanks for long durations, but significant for older facilities where truck load-outs may occur weeks apart. Ultimately, the inclusion of such models should be prioritized based on the simulation's purpose. For an analysis focused on GHG emissions and targeting methane, excluding these emissions results in minimal error. However, for an ozone or hazardous pollutant analysis, these emissions would need to be included.

In summary, mechanistic modeling modernizes emissions inventory methods for tracking and assessing methane emissions from oil and gas industry, aligning them with emerging measurement techniques, new facility designs, and expanded uses of emissions data.

# Acknowledgement

# Supporting Information Available

- PS Paper_SI.pdf: Supplementary information for the main paper

# References


(1) Intergovernmental Panel On Climate Change (Ipcc) Climate Change 2021 – The Physical Science Basis: Working Group I Contribution to the Sixth Assessment Report of the Intergovernmental Panel on Climate Change, 1st ed.; Cambridge University Press.

(2) Hanaoka, T.; Masui, T. Exploring Effective Short-Lived Climate Pollutant Mitigation Scenarios by Considering Synergies and Trade-Offs of Combinations of Air Pollutant Measures and Low Carbon Measures towards the Level of the 2 °C Target in Asia. 261, 113650.

(3) Jackson, R. B.; Saunois, M.; Bousquet, P.; Canadell, J. G.; Poulter, B.; Stavert, A. R.; Bergamaschi, P.; Niwa, Y.; Segers, A.; Tsuruta, A. Increasing Anthropogenic Methane Emissions Arise Equally from Agricultural and Fossil Fuel Sources. 15, 071002.

(4) Saunois, M. et al. The Global Methane Budget 2000–2017. 12, 1561–1623.

(5) Ganesan, A. L.; Schwietzke, S.; Poulter, B.; Arnold, T.; Lan, X.; Rigby, M.; Vogel, F. R.; Van Der Werf, G. R.; Janssens-Maenhout, G.; Boesch, H.; Pandey, S.; Manning, A. J.; Jackson, R. B.; Nisbet, E. G.; Manning, M. R. Advancing Scientific Understanding of the Global Methane Budget in Support of the Paris Agreement. 33, 1475–1512.

(6) Brown, J. A.; Harrison, M. R.; Rufael, T.; Roman-White, S. A.; Ross, G. B.;

George, F. C.; Zimmerle, D. Informing Methane Emissions Inventories Using Facility Aerial Measurements at Midstream Natural Gas Facilities. 57, 14539–14547.

(7) Saji, V. S., Umoren, S. A., Eds. Corrosion Inhibitors in the Oil and Gas Industry, 1st ed.; Wiley.

(8) Cooper, J.; Balcombe, P.; Hawkes, A. The Quantification of Methane Emissions and Assessment of Emissions Data for the Largest Natural Gas Supply Chains. 320, 128856.

(9) Peischl, J.; Ryerson, T. B.; Aikin, K. C.; De Gouw, J. A.; Gilman, J. B.; Holloway, J. S.; Lerner, B. M.; Nadkarni, R.; Neuman, J. A.; Nowak, J. B.; Trainer, M.; Warneke, C.; Parrish, D. D. Quantifying Atmospheric Methane Emissions from the Haynesville, Fayetteville, and Northeastern Marcellus Shale Gas Production Regions. 120, 2119–2139.

(10) Mitchell, A. L.; Tkacik, D. S.; Roscioli, J. R.; Herndon, S. C.; Yacovitch, T. I.; Martinez, D. M.; Vaughn, T. L.; Williams, L. L.; Sullivan, M. R.; Floerchinger, C.; Omara, M.; Subramanian, R.; Zimmerle, D.; Marchese, A. J.; Robinson, A. L. Measurements of Methane Emissions from Natural Gas Gathering Facilities and Processing Plants: Measurement Results. 49, 3219–3227.

(11) Peischl, J.; Karion, A.; Sweeney, C.; Kort, E. A.; Smith, M. L.; Brandt, A. R.; Yeskoo, T.; Aikin, K. C.; Conley, S. A.; Gvakharia, A.; Trainer, M.; Wolter, S.; Ryerson, T. B. Quantifying Atmospheric Methane Emissions from Oil and Natural Gas Production in the Bakken Shale Region of North Dakota. 121, 6101–6111.

(12) Mielke-Maday, I. et al. Methane Source Attribution in a U.S. Dry Gas Basin Using Spatial Patterns of Ground and Airborne Ethane and Methane Measurements. 7, 13.

(13) Caulton, D. R.; Shepson, P. B.; Santoro, R. L.; Sparks, J. P.; Howarth, R. W.; Ingraffea, A. R.; Cambaliza, M. O. L.; Sweeney, C.; Karion, A.; Davis, K. J.;

Stirm, B. H.; Montzka, S. A.; Miller, B. R. Toward a Better Understanding and Quantification of Methane Emissions from Shale Gas Development. 111, 6237–6242.

(14) Pétron, G. et al. A New Look at Methane and Nonmethane Hydrocarbon Emissions from Oil and Natural Gas Operations in the Colorado Denver-Julesburg Basin. 119, 6836–6852.

(15) Allen, D. T.; Cardoso-Saldaña, F. J.; Kimura, Y.; Chen, Q.; Xiang, Z.; Zimmerle, D.; Bell, C.; Lute, C.; Duggan, J.; Harrison, M. A Methane Emission Estimation Tool (MEET) for Predictions of Emissions from Upstream Oil and Gas Well Sites with Fine Scale Temporal and Spatial Resolution: Model Structure and Applications. 829, 154277.

(16) Stokes, S.; Tullos, E.; Morris, L.; Cardoso-Saldaña, F. J.; Smith, M.; Conley, S.; Smith, B.; Allen, D. T. Reconciling Multiple Methane Detection and Quantification Systems at Oil and Gas Tank Battery Sites. 56, 16055–16061.

(17) family=US EPA, g.-i., given=OAR Inventory of U.S. Greenhouse Gas Emissions and Sinks. `https://www.epa.gov/ghgemissions/inventory-us-greenhouse-gas-emissions-and-sinks`.

(18) family=US EPA, g.-i., given=OAR Greenhouse Gas Reporting Program (GHGRP). `https://www.epa.gov/ghgreporting`.

(19) Climate Change | Department of Public Health & Environment. `https://cdphe.colorado.gov/environment/air-pollution/climate-change`.

(20) Zimmerle, D.; Duggan, G.; Vaughn, T.; Bell, C.; Lute, C.; Bennett, K.; Kimura, Y.; Cardoso-Saldaña, F. J.; Allen, D. T. Modeling Air Emissions from Complex Facilities at Detailed Temporal and Spatial Resolution: The Methane Emission Estimation Tool (MEET). 824, 153653.

(21) Rutherford, J. S.; Sherwin, E. D.; Ravikumar, A. P.; Heath, G. A.; Englander, J.; Cooley, D.; Lyon, D.; Omara, M.; Langfitt, Q.; Brandt, A. R. Closing the Methane Gap in US Oil and Natural Gas Production Emissions Inventories. 12, 4715.

(22) Dawidowski, L. E.; Kolmogortseva, O.; Okazaki, T.; Person Rocha e Pinho, I.; Smyth, S. C.; Witi, J. 2019 Refinement to the 2006 IPCC Guidelines for National Greenhouse Gas Inventories. https://www.ipcc-nggip.iges.or.jp/public/2019rf/pdf/2_Volume2/19R_V2_4_Ch04_Fugitive_Emissions.pdf.

(23) Brown, J.; Harrison, M.; Rufael, T.; Roman-White, S.; Ross, G.; George, F.; Zimmerle, D. Evaluating Development of Empirical Estimates Using Two Top-down Methods at Midstream Natural Gas Facilities. https://chemrxiv.org/engage/chemrxiv/article-details/652712ca45aaa5fdbbcc6934.

(24) Festa-Bianchet, S. A.; Milani, Z. R.; Johnson, M. R. Methane Venting from Uncontrolled Production Storage Tanks at Conventional Oil Wells—Temporal Variability, Root Causes, and Implications for Measurement. 11, 00053.

(25) Allen, D. T.; Cardoso-Saldaña, F. J.; Kimura, Y. Variability in Spatially and Temporally Resolved Emissions and Hydrocarbon Source Fingerprints for Oil and Gas Sources in Shale Gas Production Regions. 51, 12016–12026.

(26) Vaughn, T. L.; Bell, C. S.; Pickering, C. K.; Schwietzke, S.; Heath, G. A.; Pétron, G.; Zimmerle, D. J.; Schnell, R. C.; Nummedal, D. Temporal Variability Largely Explains Top-down/Bottom-up Difference in Methane Emission Estimates from a Natural Gas Production Region. 115, 11712–11717.

(27) Johnson, M. R.; Conrad, B. M.; Tyner, D. R. Creating Measurement-Based Oil and Gas Sector Methane Inventories Using Source-Resolved Aerial Surveys. 4, 139.

(28) MacKay, K.; Lavoie, M.; Bourlon, E.; Atherton, E.; O'Connell, E.; Baillie, J.;

Fougère, C.; Risk, D. Methane Emissions from Upstream Oil and Gas Production in Canada Are Underestimated. 11, 8041.

(29) Cusworth, D. H.; Duren, R. M.; Thorpe, A. K.; Olson-Duvall, W.; Heckler, J.; Chapman, J. W.; Eastwood, M. L.; Helmlinger, M. C.; Green, R. O.; Asner, G. P.; Dennison, P. E.; Miller, C. E. Intermittency of Large Methane Emitters in the Permian Basin. 8, 567–573.

(30) Zhang, Y. et al. Quantifying Methane Emissions from the Largest Oil-Producing Basin in the United States from Space. 6, eaaz5120.

(31) Riddick, S. N.; Mbua, M.; Santos, A.; Hartzell, W.; Zimmerle, D. J. Potential Underestimate in Reported Bottom-up Methane Emissions from Oil and Gas Operations in the Delaware Basin. 15, 202.

(32) Barkley, Z. R.; Davis, K. J.; Feng, S.; Cui, Y. Y.; Fried, A.; Weibring, P.; Richter, D.; Walega, J. G.; Miller, S. M.; Eckl, M.; Roiger, A.; Fiehn, A.; Kostinek, J. Analysis of Oil and Gas Ethane and Methane Emissions in the Southcentral and Eastern United States Using Four Seasons of Continuous Aircraft Ethane Measurements. 126, e2020JD034194.

(33) Zimmerle, D.; Vaughn, T.; Luck, B.; Lauderdale, T.; Keen, K.; Harrison, M.; Marchese, A.; Williams, L.; Allen, D. Methane Emissions from Gathering Compressor Stations in the U.S. 54, 7552–7561.

(34) C3: Colorado Coordinated Campaign | METEC | Colorado State University. `https://metec.colostate.edu/c3/`.

(35) Zimmerle, D.; Dileep, S.; Quinn, C. Unaddressed Uncertainties When Scaling Regional Aircraft Emission Surveys to Basin Emission Estimates. 58, 6575–6585.

(36) Allen, D. T.; Pacsi, A. P.; Sullivan, D. W.; Zavala-Araiza, D.; Harrison, M.; Keen, K.; Fraser, M. P.; Daniel Hill, A.; Sawyer, R. F.; Seinfeld, J. H. Methane Emissions from

Process Equipment at Natural Gas Production Sites in the United States: Pneumatic Controllers. 49, 633–640.

(37) Plant, G.; Kort, E. A.; Brandt, A. R.; Chen, Y.; Fordice, G.; Gorchov Negron, A. M.; Schwietzke, S.; Smith, M.; Zavala-Araiza, D. Inefficient and Unlit Natural Gas Flares Both Emit Large Quantities of Methane. 377, 1566–1571.

(38) Liu, Y. et al. Assessment of Current Methane Emission Quantification Techniques for Natural Gas Midstream Applications. 17, 1633–1649.

(39) Zavala-Araiza, D.; Alvarez, R. A.; Lyon, D. R.; Allen, D. T.; Marchese, A. J.; Zimmerle, D. J.; Hamburg, S. P. Super-Emitters in Natural Gas Infrastructure Are Caused by Abnormal Process Conditions. 8, 14012.

(40) Vora, P.; Zimmerle, D. J.; Duggan, J. Use of Mechanistic Modeling to Improve Failure Mode Representation in Emissions Studies.

(41) Olugbenga, A. G.; Al-Mhanna, N. M.; Yahya, M. D.; Afolabi, E. A.; Ola, M. K. Validation of the Molar Flow Rates of Oil and Gas in Three-Phase Separators Using Aspen Hysys. 9, 327.

(42) Frankenberg, C.; Thorpe, A. K.; Thompson, D. R.; Hulley, G.; Kort, E. A.; Vance, N.; Borchardt, J.; Krings, T.; Gerilowski, K.; Sweeney, C.; Conley, S.; Bue, B. D.; Aubrey, A. D.; Hook, S.; Green, R. O. Airborne Methane Remote Measurements Reveal Heavy-Tail Flux Distribution in Four Corners Region. 113, 9734–9739.

(43) COGCC Data. `https://cogcc.state.co.us/data.html`.

(44) Visualize Summary Statistics with Box Plot - MATLAB Boxplot. `https://www.mathworks.com/help/stats/boxplot.html`.

(45) Benefits of The Tankless Production Facility - Halker Consulting. `https://www.halker.com/benefits-of-the-tankless-production-facility/`.

(46) Greenhouse Gas Reporting Rule: Revisions and Confidentiality Determinations for Petroleum and Natural Gas Systems. https://www.federalregister.gov/documents/2023/08/01/2023-14338/greenhouse-gas-reporting-rule-revisions-and-confidentiality-determinations-for-petr

(47) Lyon, D. R.; Alvarez, R. A.; Zavala-Araiza, D.; Brandt, A. R.; Jackson, R. B.; Hamburg, S. P. Aerial Surveys of Elevated Hydrocarbon Emissions from Oil and Gas Production Sites. 50, 4877–4886.

# TOC Graphic